



## OPEN ACCESS

EDITED BY  
Tingting Liu,  
Xi'an Polytechnic University, China

REVIEWED BY  
Rakesh Kumar,  
Nalanda University, India  
Zhichong Qi,  
Henan University, China

\*CORRESPONDENCE  
Jun Meng,  
✉ mengjun1217@syau.edu.cn  
Wenfu Chen,  
✉ wfchen5512@163.com

SPECIALTY SECTION  
This article was submitted to Toxicology,  
Pollution and the Environment,  
a section of the journal  
Frontiers in Environmental Science

RECEIVED 03 December 2022  
ACCEPTED 21 December 2022  
PUBLISHED 06 January 2023

CITATION  
Zhang W, Meng J, Huang Y, Sarkar B,  
Singh BP, Zhou X, Gao J, Teng Y, Wang H  
and Chen W (2023), Effects of soil grain  
size and solution chemistry on the  
transport of biochar nanoparticles.  
*Front. Environ. Sci.* 10:1114940.  
doi: 10.3389/fenvs.2022.1114940

COPYRIGHT  
© 2023 Zhang, Meng, Huang, Sarkar,  
Singh, Zhou, Gao, Teng, Wang and Chen.  
This is an open-access article distributed  
under the terms of the [Creative Commons  
Attribution License \(CC BY\)](https://creativecommons.org/licenses/by/4.0/). The use,  
distribution or reproduction in other  
forums is permitted, provided the original  
author(s) and the copyright owner(s) are  
credited and that the original publication in  
this journal is cited, in accordance with  
accepted academic practice. No use,  
distribution or reproduction is permitted  
which does not comply with these terms.

# Effects of soil grain size and solution chemistry on the transport of biochar nanoparticles

Wenke Zhang<sup>1,2</sup>, Jun Meng<sup>1,2\*</sup>, Yuwei Huang<sup>1,2</sup>, Binoy Sarkar<sup>3</sup>,  
Bhupinder Pal Singh<sup>4</sup>, Xuanwei Zhou<sup>1,2</sup>, Jian Gao<sup>1,2</sup>,  
Yunpeng Teng<sup>1,2</sup>, Hailong Wang<sup>5</sup> and Wenfu Chen<sup>1,2\*</sup>

<sup>1</sup>National Biochar Institute of Shenyang Agricultural University, Shenyang, China, <sup>2</sup>Key Laboratory of Biochar and Soil Improvement, Ministry of Agriculture and Rural Affairs, Shenyang, China, <sup>3</sup>Future Industries Institute, University of South Australia, Mawson Lakes, SA, Australia, <sup>4</sup>School of Environmental and Rural Science, University of New England, Armidale, NSW, Australia, <sup>5</sup>School of Environmental and Chemical Engineering, Foshan University, Foshan, Guangdong, China

Biochar nanoparticles (BC-NP) have attracted significant attention because of their unique environmental behavior, some of which could potentially limit large-scale field application of biochar. Accurate prediction of the fate and transportability of BC-NP in soil matrix is the key to evaluating their environmental influence. This study investigated the effects of soil grain size and environmentally relevant solution chemistry, such as ionic strength (cation concentration, 0.1 mM–50 mM; cation type, Na<sup>+</sup>, and Ca<sup>2+</sup>), and humic acid (HA; 0–10 mg/L), on the transport behavior of BC-NP *via* systematic column experiments. The transportability of BC-NP in the soil-packed column decreased with decreasing soil grain size and was inversely proportional to soil clay content. At low cation concentrations (0.1–1.0 mM), a considerable proportion of BC-NP (15.95%–67.17%) penetrated the soil columns. Compared with Na<sup>+</sup>, Ca<sup>2+</sup> inhibited the transportability of BC-NP in the soil through a charge shielding effect. With increasing HA concentration, the transportability of BC-NP increased, likely due to an enhanced repulsion force between BC-NP and soil particles. However, at a high HA concentration (10 mg/L), Ca<sup>2+</sup> bridging reduced the transportability of BC-NP in the soil. Breakthrough curves of BC-NP were explained by the two-site kinetic retention model. The antagonistic effects of ionic strength and HA indicated that the transport behavior of BC-NP in the soil was governed by competitive effects of some environmental factors, including soil grain size, environmental solution chemistry, and natural organic matter content.

## KEYWORDS

soil textural composition, ionic strength, humic acid, soil column, solution chemistry

## 1 Introduction

Biochar is a carbon-rich solid product produced by the thermal decomposition of biomass at relatively low temperatures, mostly <700°C, in absence of oxygen (Ippolito et al., 2020; Wu et al., 2021). Biochar has been widely used in carbon sequestration, soil nutrient retention, and environmental remediation purposes (Chen et al., 2019; Chen et al., 2022; Liu et al., 2022). As an important part of biochar, biochar nanoparticles (BC-NP) have attracted much attention due to their wide application in adsorbents, sensors, capacitors, and photocatalytic materials (Tan et al., 2016; Ramanayaka et al., 2020; Zhang et al., 2022). However, these small biochar particles are reactive and could leach into surface water and soil profile *via* runoff, irrigation, and infiltration (Ramanayaka et al., 2020; Wu et al., 2022). BC-NP may contain organic pollutants (Song et al., 2019) and have a high adsorption affinity for environmental pollutants (Naghdi

et al., 2019; Swaren et al., 2022), facilitating transport or co-transport with pollutants to the groundwater system, which could result in potential environmental risks (Lian et al., 2020; Swaren et al., 2022). Therefore, a complete understanding of the fate and transport behavior of BC-NP in the environment is crucial for optimizing biochar's utilization and assessing potential risk in agriculture and environmental remediation applications.

Multiple column simulation experiments were previously performed to investigate the effects of hydraulic, porous media properties, solution chemistry, physicochemical properties, and mineral coating of BC-NP on the transport and retention of BC-NP in porous media (Chen et al., 2017; Wang et al., 2019; Liu et al., 2021). The results of these studies showed that BC-NP had high transportability in porous media with low ionic strength and high pore water velocity, or in the presence of natural organic compounds and surfactants. Although these studies have greatly advanced the understanding of retention and transport mechanisms of BC-NP in porous media, BC-NP transport behavior in natural soils is far from complete comprehension, which limits the ability to predict and monitor the transport and fate of BC-NP in the environment.

Natural soil is a complex heterogeneous system, and its solution chemistry, textural composition (sand, silt, and clay content), surface roughness, organic matter content, and other properties can significantly affect the transportability of nanoparticles (Liang et al., 2021; Cao et al., 2022). Therefore, the transport of nanoparticles in well-defined model porous media (e.g., quartz sand, glass bead) may be less suitable for predicting the actual mobility of BC-NP in natural soils. Previous studies showed that after adding electrolyte into a colloidal system, the electric double layer of colloidal particles will be compressed, and the electrostatic repulsion between nanoparticles will be reduced, thus reducing the stability of the nanoparticles (Yang et al., 2019; Cao et al., 2022). Since soil solution usually contains different concentrations and types of electrolytes, and BC-NP may be surface-modified by natural organic matter during the transport process, the transport behavior of BC-NP in natural soil is complicated. Only a limited number of studies have investigated the effect of solution chemistry on BC-NP fate and transport in natural soil.

In studying the transport of nanoparticles in the environmental matrix, the grain size of media could also play an important role (Zhang et al., 2022; Mlih et al., 2022). Based on filtration theory, if all factors affecting the transport behavior of nanoparticles are kept constant, grain size of porous media increase can lead to a decrease in the single-collector contact efficiency (Yao et al., 2002). This is due to the larger grained porous media providing less surface area for the nanoparticles to deposit (Xin et al., 2021). The maximum solid phase concentration of retained nanoparticles has also been observed to increase with a decrease in porous media grain size (Liang et al., 2013). In addition, finer grains may create smaller pores in porous media to increase the possibility of physical straining (Xin et al., 2016). All these factors indicate that nanoparticle retention is expected to increase in finer-grained porous media. Conversely, some studies also indicated that grain size of porous media had little effect on the transport of nanoparticles (Tian et al., 2011). The aforementioned studies investigating the transportability of nanoparticles show that their transport behavior is sensitive to the grain size of porous media, but no study to date investigated the impact of soil grain size on BC-NP transport behavior.

We hypothesized that ionic strength (cationic concentration and cationic type) affects the transportability of BC-NP in soil at

environmentally relevant solution conditions, and that soil grain size further alters transportability of BC-NP and affects the interactions between cation and BC-NP. Besides, we also hypothesized that the humic acid (HA) ubiquitous in soil influences the transportability of BC-NP as well as the interactions between ionic strength and soil grain size. To test our hypotheses, soil particles graded by grain size were packed into the plexiglass column to make the soil-packed column. Subsequently, solutions with different concentrations of NaCl, CaCl<sub>2</sub>, and HA were used as background solutions to explore cationic concentration, cationic type, HA concentration, and soil grain size effects on transportability of BC-NP in soil. The breakthrough curves (BTC) of BC-NP in soil were fitted to further analyze the underlying mechanisms. The objectives of this study are: (1) to determine the effect of different cationic concentrations, types, and concentrations of HA on the transport and retention of BC-NP in soil, and (2) to assess the impact of soil grain size on the transport and retention of BC-NP in soil, and (3) employ a mathematical model to simulate the transport behavior of BC-NP in soil.

## 2 Materials and methods

### 2.1 Preparation of soil media and BC-NP suspensions

Soil samples used in the BC-NP column transport experiments (described in section 2.3) were taken from the surface layer (0–30 cm) of the long-term experimental paddy field of Shenyang Agricultural University in Liaoning Province (41°49'3" N, 123°33'49" E), China. The field has been used to grow a single rice crop for over 50 years. Five sub-samples were randomly collected before the spring plowing in April 2021, and visible plant residues and stones were manually removed. In order to investigate the effect of soil grain size on the transport of BC-NP by minimizing the variation due to other soil properties (e.g., pH, soil total organic carbon content), the sampled soil was air-dried, ground, and passed through 10, 18, 35, and 60 mesh sieves sequentially to obtain three size grades (10–18 mesh, 1290.0 μm median grain size; 18–35 mesh, 652.5 μm median grain size; 35–60 mesh, 337.5 μm median grain size). Selected physicochemical properties of the sampled soil were determined, and the results are shown in Supplementary Table S1.

NaCl and CaCl<sub>2</sub> were used as the electrolytes in the background solution as Na<sup>+</sup> Ca<sup>2+</sup> are abundant and omnipresent in the soil matrix. There is a simple linear relationship between the ionic strength ( $I_c$ ) and the electrical conductivity (EC) value ( $I_c = 0.0127 \times EC$ ) of a solution (Morrison et al., 1990). The average EC values of sampled soil, rainwater, and groundwater were 35.2 μs/cm, 26.6 μs/cm, and 836.6 μs/cm, respectively (Supplementary Table S2). To be close to the ionic strength of the soil solution and take into account its buffering capacity, the minimum concentration of NaCl and CaCl<sub>2</sub> background solution in this experiment was set to 1.0 mM and 0.1 mM, respectively. Concentrations of other background solutions (10 and 50 mM NaCl; 0.5 and 1.0 mM CaCl<sub>2</sub>) referred to the minimum concentration of NaCl and CaCl<sub>2</sub>. Meanwhile, to study the effect of HA on the transport behavior of BC-NP in the soil matrix, 5.0 and 10 mg/L HA (purchased from Sigma-Aldrich) were

TABLE 1 Mass balance percentages of BC-NP at different experimental conditions.

Exp No.	Soil Mesh	Background solutions	Mass balance of BC-NP (%) <sup>a</sup>	
			Efflux rate	Retention rate
1	10–18	1.0 mM NaCl	67.17 ± 3.98 a <sup>b</sup>	33.09 ± 1.13 i
2	10–18	10 mM NaCl	4.24 ± 1.48 i	94.55 ± .94 c
3	10–18	50 mM NaCl	2.20 ± 1.12 j	96.86 ± .58 b
4	10–18	.1 mM CaCl <sub>2</sub>	36.05 ± 2.30 c	64.50 ± 1.84 h
5	10–18	.5 mM CaCl <sub>2</sub>	1.49 ± 1.02 k	97.66 ± .48 ab
6	10–18	1.0 mM CaCl <sub>2</sub>	.88 ± .84 lm	100.33 ± 2.67 a
7	18–35	1.0 mM NaCl	38.20 ± 2.58 b	63.84 ± 1.30 h
8	18–35	10 mM NaCl	1.48 ± .98 k	99.46 ± 1.81 a
9	18–35	50 mM NaCl	.20 o ± .25 o	97.35 ± .67 ab
10	18–35	.1 mM CaCl <sub>2</sub>	30.97 ± 2.26 d	68.35 ± 1.75 g
11	18–35	.5 mM CaCl <sub>2</sub>	.91 ± .93 l	102.89 ± 2.19 a
12	18–35	1.0 mM CaCl <sub>2</sub>	.54 ± .39 n	99.09 ± 1.20 a
13	35–60	1.0 mM NaCl	23.77 ± 1.98 e	77.28 ± 2.21 f
14	35–60	10 mM NaCl	.83 ± .80 m	96.20 ± .66 b
15	35–60	50 mM NaCl	.20 o ± .29 o	101.77 ± 2.39 a
16	35–60	.1 mM CaCl <sub>2</sub>	15.95 ± 1.66 gh	77.84 ± 1.67 f
17	35–60	.5 mM CaCl <sub>2</sub>	1.34 ± .93 k	97.11 ± .48 ab
18	35–60	1.0 mM CaCl <sub>2</sub>	.62 ± .71 n	101.70 ± 2.21 a
19	10–18	10 mM NaCl + 5.0 mg/L HA <sup>c</sup>	17.16 ± 1.80 g	84.10 ± .94 e
20	10–18	10 mM NaCl + 10 mg/L HA	29.17 ± 2.07 d	69.96 ± .84 g
21	10–18	.5 mM CaCl <sub>2</sub> + 5.0 mg/L HA	20.78 ± 1.85 f	79.55 ± 1.84 f
22	10–18	.5 mM CaCl <sub>2</sub> + 10 mg/L HA	14.19 ± 1.62 h	88.16 ± 1.57 d

<sup>a</sup>Efflux rate and retention rate of BC-NP, recovered from column experiments.

<sup>b</sup>The presented values are the mean ± standard deviation ( $n = 3$ ). Mean values at different experimental conditions followed by the same lowercase letters are not significantly different using LSD, test at  $p < 0.05$ .

<sup>c</sup>HA, stands for humic acid.

dissolved in 10 mM NaCl and 0.5 mM CaCl<sub>2</sub> to prepare background solutions.

The BC-NP used in this experiment was purchased from Hainuo Charcoal Co., Ltd. (Shanghai, China). The BC-NP was made from coconut shells through high-temperature carbonization and nano-scale ultra-fine grinding. Selected physicochemical properties of the BC-NP were determined, and the results are shown in [Supplementary Table S3](#). The suspensions of BC-NP (200 mg/L) containing desired concentrations of NaCl, CaCl<sub>2</sub>, and HA were prepared for subsequent experiments ([Table 1](#)).

The  $\zeta$ -potential values of sampled soils in the desired background solutions were determined using a Zetasizer analyzer (Nano ZS ZEN3600, Malvern, United Kingdom). The soil suspension was prepared by suspending a certain amount of sampled soil in desired background solutions, followed by sonication for 30 min and stand for 5 h ([Supplementary Table S4](#)).

## 2.2 Colloidal stability of BC-NP

Colloidal stability of BC-NP in desired solution chemistry conditions was assessed by measuring temporal changes of BC-NP suspension concentration. The prepared BC-NP suspensions (200 mg/L) were stirred and sonicated for 10 min to disperse the BC-NP completely. A colloidal stability experiment of BC-NP was carried out for a total of 780 min, and 2 mL suspension was sampled every 10 min within 1 h after the start of experiment, followed by a sample every 30 min. All measurements were run in triplicate, and the average values and standard deviations are shown in [Figure 1](#). The concentration (C) of BC-NP in suspension was determined *via* a UV-Vis spectrophotometer (UV5Bio, Mettler Toledo, China) at the wavelength of 288 nm, and the details of the analysis can be found in the [Supplementary Section S4](#).

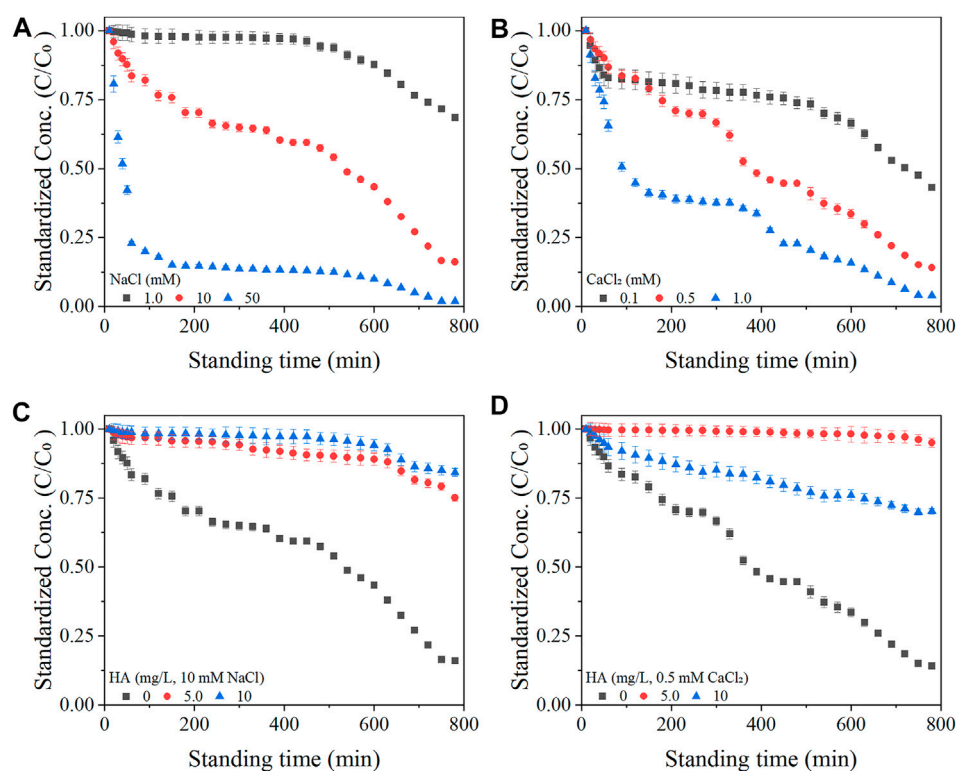


**FIGURE 1**

Colloidal stability of biochar nanoparticles (BC-NP) (expressed as standardized concentration of  $C/C_0$ ,  $C$  and  $C_0$  are the real-time and initial concentration of influx respectively) at varying concentrations of NaCl [1.0, 10, and 50 mM; (A)],  $\text{CaCl}_2$  [0.1, 0.5, and 1.0 mM; (B)], and HA (0, 5.0, and 10 mg/L) in the presence of 10 mM NaCl (C) or 0.5 mM  $\text{CaCl}_2$  (D). Error bars represent the standard deviation of means ( $n = 3$ ).

## 2.3 Column experiments

Column experiments with BC-NP were executed at saturated flow condition. Multiple plexiglass columns (inner diameter 2 cm, length 16 cm) were uniformly packed separately with 8 cm air-dried soil of 10–18, 18–35, and 35–60 mesh grain size. A 75  $\mu\text{m}$  nylon net was placed at the bottom of the column to support the soil above. Deionized distilled water was added from the bottom of the column and gradually moved upward through the entire column to remove any air pockets, and then the saturated soil columns were leached by gravity with at least 200 mL  $\text{CaCl}_2$  (20 mM). When the absorbance of the effluent at 800 nm was less than 0.001, the soil colloids in the column were considered to be stable and used for subsequent experiments.

After the soil colloid stabilization step was completed, a peristaltic pump (DG-2, Baoding Longer Precision Pump Co., Ltd., China) was used to introduce a top-down flow of the non-reactive tracer and desired solution into the column. Firstly, 6 pore volumes (PVs) of 1 mM non-reactive tracer (NaBr) were injected into the soil-packed column to obtain the dispersion coefficient and average pore-water velocity by fitting BTC of NaBr using the STANMOD code (Supplementary Section S5). Then, the influx was switched back to the background solution to elute the tracer thoroughly. A pre-prepared BC-NP suspension was then pumped into the soil-packed column. During this period, the BC-NP suspension was perpetually stirred to prevent it from aggregation. After 8 PV suspensions passed through the soil column, the corresponding background solution

without BC-NP was pumped at the same conditions until BC-NP was not detected in the efflux. Referring to the experimental design of Fang et al. (2009), an 8 cm constant water head was maintained, and gravity flow was used for leaching throughout the experiment. Efflux samples were collected at certain intervals *via* a fraction collector (BSZ-100, Shanghai Huxi Analysis Instrument Factory Co., Ltd.). All experiments were performed at room temperature ( $25^\circ\text{C} \pm 1^\circ\text{C}$ ) and performed in triplicate. Supplementary Table S4 gives detailed properties of the soil-packed columns.

Concentrations of BC-NP in efflux and influx were defined as  $C_L$  and  $C_0$ , respectively. The BTC was defined as a function of the PV's standardized concentration ( $C_L/C_0$ ).  $C_{\text{max}}$  was defined as the maximum value of  $C_L/C_0$  in BTC. The average hydrodynamic radius and  $\zeta$ -potential of BC-NP in the influx and efflux were measured using a Zetasizer analyzer (Nano ZS ZEN3600, Malvern, United Kingdom).

After completing the column transport experiments, retention curves (RC) of BC-NP in the soil-packed columns were determined. Briefly, the soil sample inside the column was recovered and divided into eight segments in 1.0 cm increments. The contents of BC-NP in the soil were measured according to Chen et al. (2017), and details of the method can be found in the Supplementary Section S6. The efflux rate and retention rate of BC-NP in the column experiments were calculated by calculating the mass of BC-NP in the efflux and soil (Supplementary Table S1). Correlation analysis was conducted to study the relationship between the retention rate of BC-NP and soil properties. Details can be found in the Supplementary Section S7.

## 2.4 Data analysis

To qualitatively understand the transport behavior of BC-NP in soil, this study adopted the classical Derjaguin-Landau-Verwey-Overbeek (DLVO) theory, which considered that the interaction energy between BC-NP and soil particles was the sum of van der Waals attraction and electrostatic double layer repulsion (Wang et al., 2022). The sphere-plate model was used for calculation, and detailed equations and calculation processes are given in the [Supplementary Section S8](#).

The one-dimensional form of the convection-dispersion equation (CDE) model with two kinetic adsorption sites was used to simulate the transport of BC-NP through the soil column (Bradford et al., 2003). The two-site kinetic retention model described the transport of BC-NP between aqueous and solid phases. The first kinetic site (site 1) assumed the reversible retention using first-order attachment ( $k_1$ ) and detachment ( $k_{1d}$ ) rate coefficients, respectively. The second kinetic site (site 2) assumed irreversible and time-dependent retention, as described by the Langmuirian blocking (Adamczyk et al., 1994), using a second-order attachment coefficient ( $k_2$ ) and the maximum solid-phase concentration ( $S_{2max}$ ) of BC-NP. Detailed equations and calculation processes of the CDE model are given in the [Supplementary Section S9](#).

## 2.5 Statistical analysis

The LSD (Least-Significant Difference) test was used for one-way ANOVA (Analysis of Variance) to determine the statistically significant differences and Pearson correlation analysis was used to determine the correlation in measurement parameters. SPSS18.0 software was used for statistical analysis, and the mean difference was statistically significant when  $p < 0.05$ .

## 3 Results and discussion

### 3.1 Properties of soil samples and BC-NP suspensions

The physicochemical properties of the soil samples are shown in [Supplementary Table S1](#), respectively. The soils of the three grades were neutral in reaction (average pH = 6.9), and the soil total organic carbon content was 11.0–11.3 g/kg. There were significant differences in the textural composition of three soil grades. For example, the clay content of soil increased significantly with the mesh of soil.

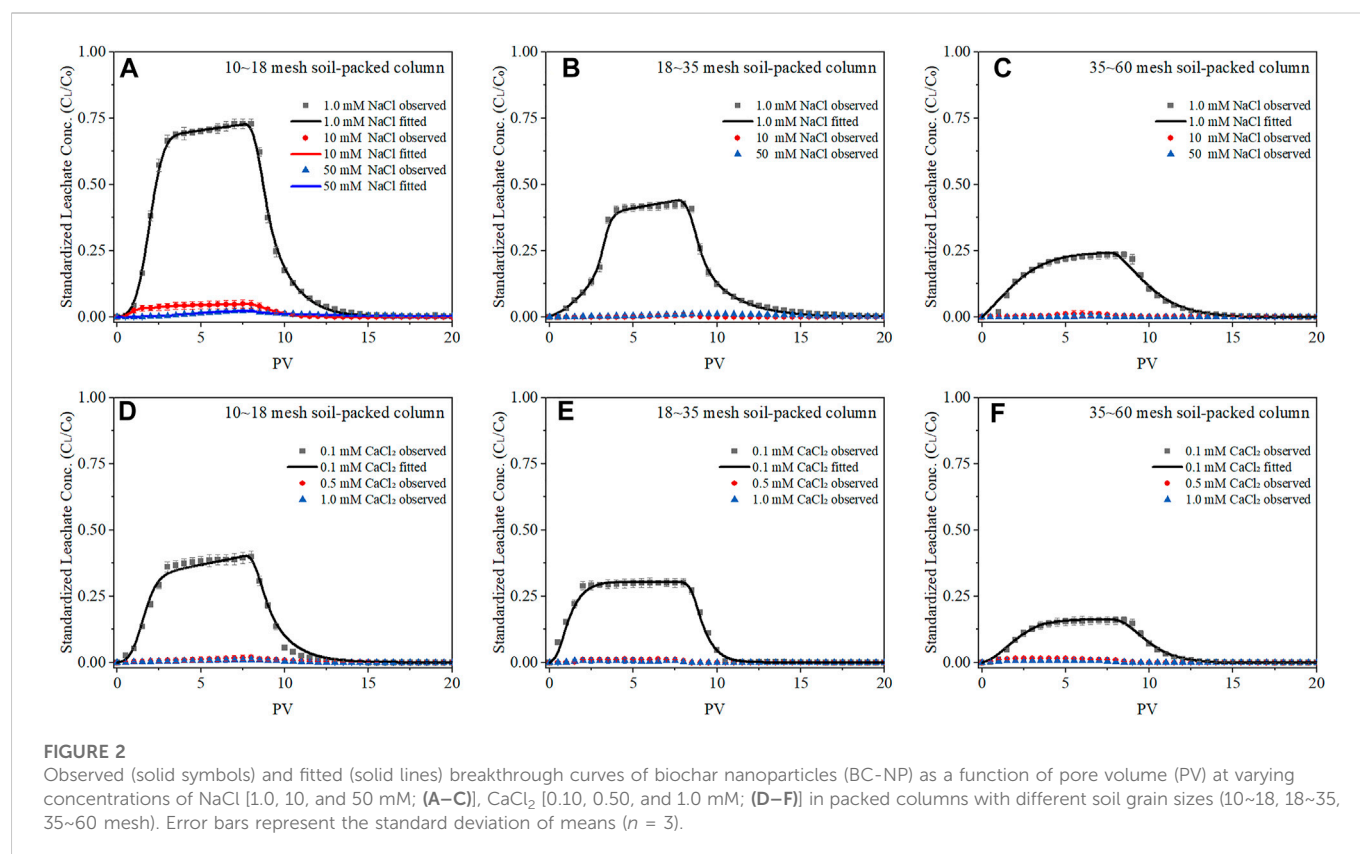
The hydrodynamic radii of BC-NP were between 284.71 nm and 488.77 nm in the experimental suspensions, 1-order of magnitude larger than the grain size ([Supplementary Tables S3, S5](#)). These findings suggested a homogeneous aggregation of BC-NP in desired background solutions. [Figures 1A, B](#) show that the BC-NP concentration decreased with increasing cationic concentration, which meant that the hydrodynamic radii of BC-NP increased with increasing cationic concentration. Other studies also reported similar phenomena (Chen et al., 2017). With the increase of ionic concentration, homogeneous aggregation was likely to occur due to the compressed electrical double layers on the surface of colloidal particles, and the electrostatic repulsion (i.e., its ability to resist homogeneous aggregation) between the colloidal particles decreased

(Chen et al., 2017; Xu et al., 2017). Compared with the same concentration of  $\text{Na}^+$ , when the suspension contains  $\text{Ca}^{2+}$ , the charge shielding effect will occur, which reduced the electrostatic repulsion between the colloidal particles and further reduced the stability of the colloidal particles (Wang et al., 2008). HA could adsorb on the surface of nanoparticles, and change the specific surface area, steric resistance, and electrostatic repulsion, thus improving the dispersion and stability of colloidal particles (Lozano and Berge, 2012; Gui et al., 2021). As expected, HA increased the colloidal stability of BC-NP in NaCl or  $\text{CaCl}_2$  solution, and at least 70% of the BC-NP remained in suspension of the given solution chemistry after standing for 780 min ([Figures 1C, D](#)).

### 3.2 Effect of cationic concentration and type on the transport of BC-NP

The BTCs of BC-NP in the soil-packed columns are shown in [Figure 2](#), and the calculated transport parameters are listed in [Table 1](#). The increase of background solution's concentration significantly affected the transportability of BC-NP. For example, in the column packed with 10–18 mesh soil, when NaCl concentration increased from 1.0 mM to 50 mM, the  $C_{max}$  of BC-NP decreased from 0.729 to 0.024, and the efflux rate decreased from 67.17% to 2.20% ([Figure 2A; Table 1](#)). This showed that the transportability of BC-NP in soil decreased with the increase in cationic concentration. The electrical double layers theory can explain this. An increased ionic concentration can compress the electrical double layer thickness of colloidal particles and reduce the electrostatic repulsion between the colloidal particles, thus facilitating the formation of larger aggregates and inhibiting the transportability of colloidal particles by the size-selective effect of the porous media (Feriancikova and Xu, 2012; Mlih et al., 2022). In addition, these results could also be explained by the DLVO interaction energy calculations. The repulsive energy barrier ( $\Phi_{max}$ ) between colloidal particles and porous media will decrease with an increase in solution ionic strength, which is beneficial to the deposition/retention of colloidal particles (Faibish et al., 1998; Chen et al., 2017). For example, when the concentration of NaCl increased from 1.0 to 50 mM in 10–18 mesh soil-packed column, the  $\Phi_{max}$  decreased from 498.90  $k_B T$  (where  $k_B$  is the Boltzmann constant and  $T$  is the absolute temperature) to 228.78  $k_B T$  ([Figure 3A; Supplementary Table S6](#)).

For a given cationic concentration, the effect of  $\text{Ca}^{2+}$  ion on the transportability of BC-NP was stronger than that of  $\text{Na}^+$  ion. For example, when the background solution was 1.0 mM NaCl, the  $C_{max}$  of BC-NP in 18–35 mesh soil-packed column was 0.425, while the  $C_{max}$  was only 0.008 with 1.0 mM  $\text{CaCl}_2$  ([Figures 2B, E](#)). The difference in BC-NP transport behavior between the two cations can be attributed to the more substantial charge neutralization by bivalent cations than monovalent cations, since  $\zeta$ -potentials of BC-NP and soils were significantly higher in  $\text{CaCl}_2$  than in NaCl ([Supplementary Tables S4, S5](#)). This effect is well known, and studies of other nanoparticles (e.g., plastic nanoparticles) previously observed the above phenomena (Braun et al., 2015; Wu et al., 2020). The DLVO theory can further verify the above results. For example, when the background solution was 1.0 mM NaCl, the  $\Phi_{max}$  was 503.40  $k_B T$  in 18–35 mesh soil-packed column, which was significantly higher than that of 82.00  $k_B T$  with 1.0 mM  $\text{CaCl}_2$  ([Supplementary Table S6](#)). The results showed that at comparable conditions,  $\text{Ca}^{2+}$  ions in the system decreased the



mutual repulsion energy between BC-NP and soil particles, thereby weakening the transportability of BC-NP.

### 3.3 Effect of soil grain size on the transport of BC-NP

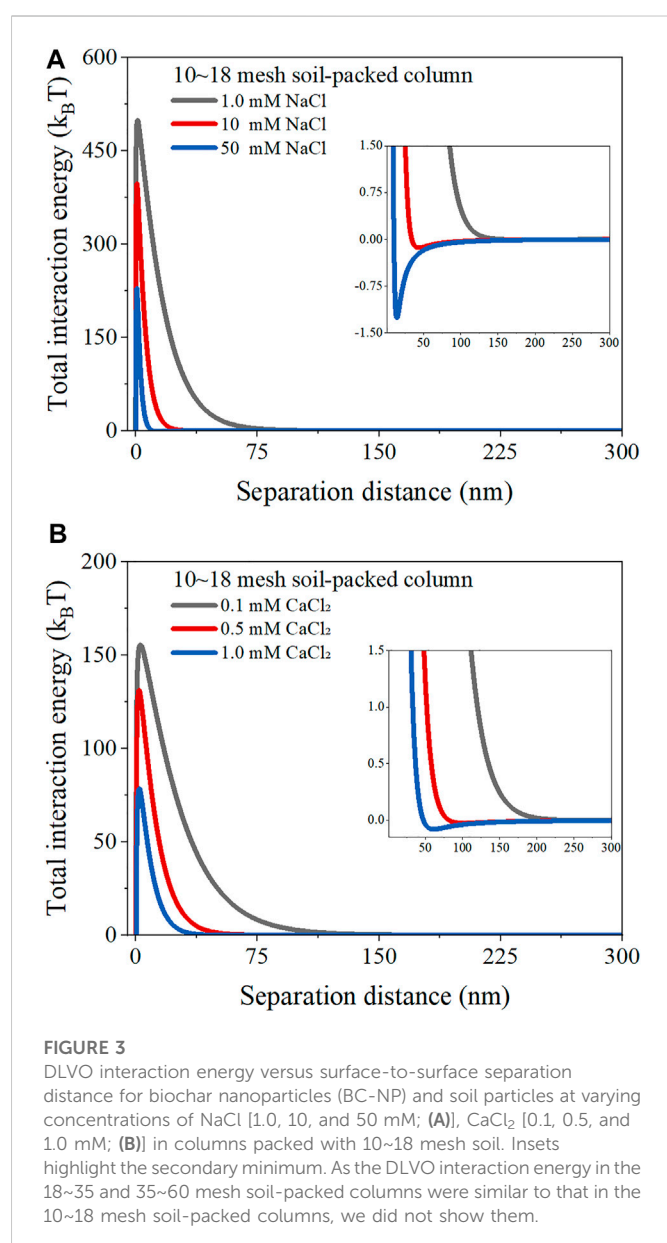
With a similar background solution, the decrease in soil grain size greatly diminished the transportability of BC-NP (Figure 2). For example, when the background solution was 0.1 mM CaCl<sub>2</sub>, the  $C_{max}$  and efflux rate of BC-NP in 10–18 mesh soil-packed column were 0.399% and 36.05%, while the  $C_{max}$  and efflux rate were 0.302% and 30.97% in 18–35 mesh soil-packed column (Figures 2D, E; Table 1). This can partially be explained by an increasing rate of mass transfer to the collector surface with a decrease in collector size as predicted by filtration theory (Kamrani et al., 2018; Xin et al., 2021).

### 3.4 Retention curve of BC-NP in soil-packed column

To better understand the transport behavior of BC-NP in the soil-packed columns, corresponding RC were determined (Figure 4). The RC's shape suggested that BC-NP decreased exponentially or hyper exponentially with increasing soil depth. That is, there was a greater retention of BC-NP in the column inlet, and decreased rapidly with depth. Some scholars have pointed out that the non-monotonic retention curve may be related to the agglomeration process and heterogeneity of colloids, and may also related to the sieving of porous media (Bradford et al., 2003; Bradford and Leij, 2018). Similar RC have

been observed for BC-NP in quartz sand and soil packed columns (Wang et al., 2013; Chen et al., 2017). BC-NP were concentrated in the surface soil (0–2 cm), which became more obvious with an increased cationic concentration or cationic valence state in the background solution. For example, when the background solution was 1.0 mM NaCl, the retention of BC-NP in the surface soil accounted for 33.38% of the total retention in the 10–18 mesh soil-packed column, and this value increased to 85.58% and 96.72% when the NaCl concentration increased to 10 mM and background solution was 1.0 mM CaCl<sub>2</sub> respectively (Figures 4A, B).

Several potential mechanisms could explain the retention of colloidal particles in porous media, which include heterogeneity of size and surface charge of colloidal particles and porous media, secondary minimum ( $\Phi_{2min}$ ), physical straining, media surface roughness, nanoparticle aggregation, and so on (Torkzaban et al., 2008; Petosa et al., 2010; Porubcan and Xu, 2011). In the present study, heterogeneity of grain size and charge distribution of BC-NP and soil particles might be the key mechanisms behind a monotonically decreasing RC. The iron and aluminum oxides in paddy soil are expected to be positively charged at the experimental pH values (~8) in this study (Wu et al., 2020). Soil clay minerals such as montmorillonite and kaolin also have positively charged edges (Wang et al., 2014a). Thus, these positive sites of soil will affect the transportability of negatively charged BC-NP. This study monitored the  $\zeta$ -potential and hydrodynamic radius of BC-NP in the influx and efflux. Supplementary Table S5 showed that the absolute value of  $\zeta$ -potential of BC-NP decreased after flowing through the soil-packed columns, indicating that BC-NP with a higher negative charge and smaller grain size was adsorbed on the positively charged sites of the soil. In general, the absolute value of  $\zeta$ -potential of nanoparticles with



small grain size is larger than that of large size grains at identical conditions (Wang et al., 2013; Chen et al., 2017).

Furthermore, since the  $\Phi_{2\text{min}}$  is gravitational potential energy in this study, BC-NP is more likely to be trapped in it with the increase of cationic concentration or cationic valence state. For example, in the 10–18 mesh soil-packed column, when the concentration of NaCl increased from 1.0 mM to 50 mM, the  $\Phi_{2\text{min}}$  between BC-NP and soil colloids decreased from  $-0.0074$  to  $-1.2618$   $k_B T$  (Figure 3A, Supplementary Table S6), which was in accordance with the trend of BC-NP retention (Table 1). What's more, the hydrodynamic radius of BC-NP in the influx was larger than BC-NP in the efflux (Supplementary Table S5), which resulted from the size-selective effect of the porous media (Wang et al., 2015). This observation further confirmed that BC-NP had been homogeneously aggregated during flowing through the soil (Fang et al., 2009). In addition, BC-NP aggregation was pronounced at higher concentration of background solution (Figure 1 and Supplementary Table S5),

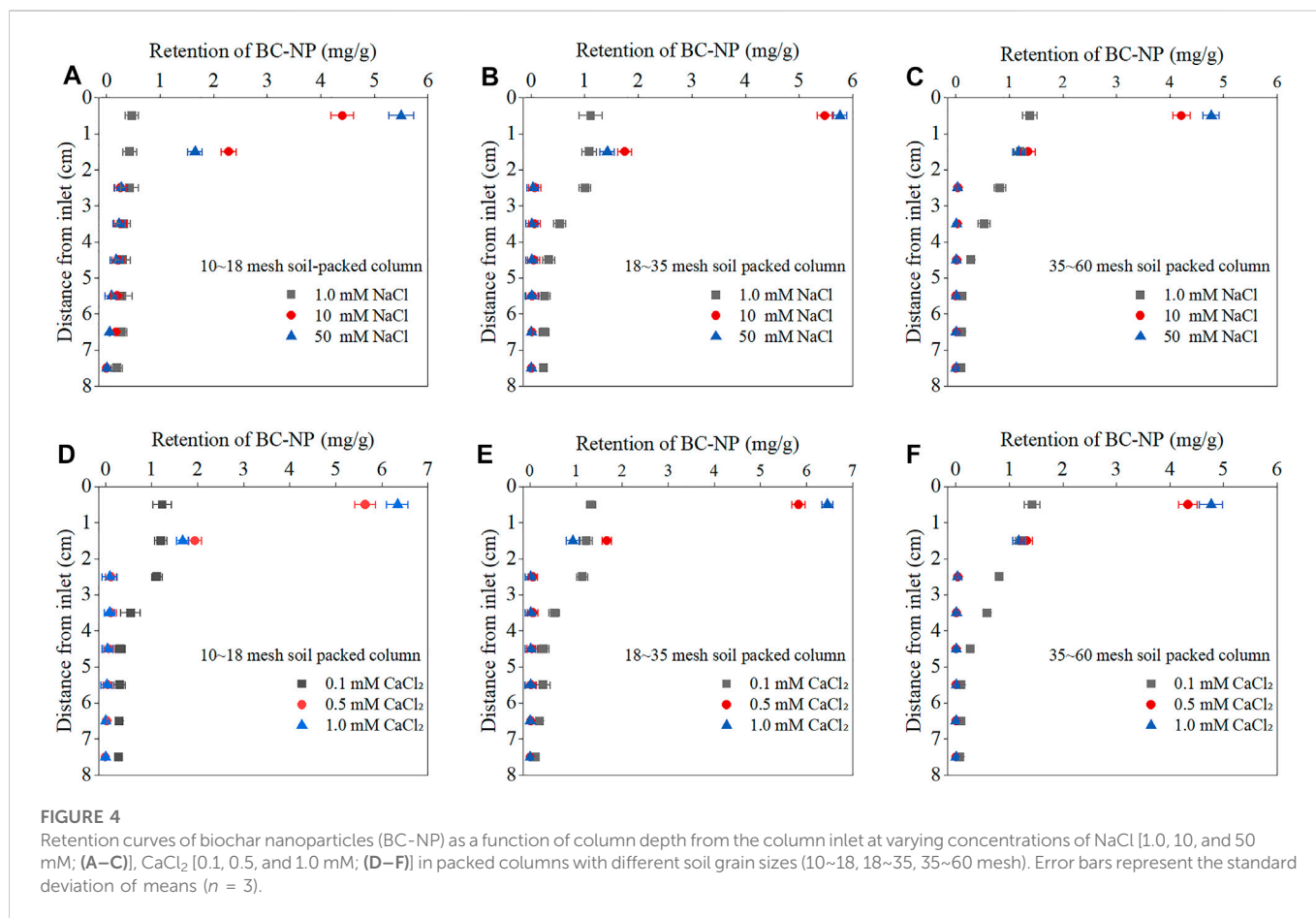
resulting in the hyper exponential shape of RC (Figure 4) and almost BC-NP (>98.5%) retaining in surface soil of 18–35 and 35–60 mesh soil-packed columns with medium (10 mM NaCl and 0.5 mM CaCl<sub>2</sub>) and high (50 mM NaCl and 1.0 mM CaCl<sub>2</sub>) concentrations of background solution (Figure 4).

Alternatively, retention of BC-NP was closely related to the grain size of porous media. At identical background solution conditions, with a decrease in soil grain size, retention of BC-NP in the surface soil (0–2 cm) increased. For example, when the background solution was 0.1 mM CaCl<sub>2</sub>, retention of BC-NP in the surface soil accounted for 45.73% of the total retention in the 10–18 mesh soil-packed column, while this value increased to 57.50% in the 35–60 mesh soil-packed column (Figures 4D, F). This can partially be explained by the fact that with a decrease in grain size of porous media and an increase in specific surface area, the mass transfer rate of colloidal particles and collectors (soil particles) will increase, according to the colloid filtration theory (Kamrani et al., 2018). BC-NP retention rate decrease with an increase in soil grain size (Table 1), resulting in less contact with the retention sites on the soil particles and thus high transportability of BC-NP in the columns. Furthermore, released clay particles from soil could form smaller pores and retain BC-NP by physical straining. In this case, BC-NP could be trapped in small pores of clay, restricting BC-NP transport, especially when the ratio of nanoparticles to media particles diameter ( $D_p/D_s$ ) is greater than 0.002 (Bradford et al., 2002; Fang et al., 2009). In the present study, almost all  $D_p/D_s$  values of 35–60 mesh soil-packed columns were higher than the critical value of 0.002, indicating that the physical straining effect occurred during the transport of BC-NP through the 35–60 mesh soil-packed columns (Supplementary Table S4). The transportability of BC-NP was therefore affected by the soil textural composition, especially the sand and clay content. This could also explain that the retention rate of BC-NP was positively correlated with clay (grain size, <2  $\mu\text{m}$ ) content and negatively correlated with sand (grain size, 20–2000  $\mu\text{m}$ ) content of soil, as described in Supplementary Table S7.

### 3.5 Effect of HA on the transport of BC-NP

The BTC and RC of BC-NP in the soil-packed columns with different HA contents are shown in Figures 5A–D. The overall transportability of BC-NP increased in the presence of HA. For example, when the background solution was 10 mM NaCl and the concentration of HA increased from 0 mg/L to 10 mg/L, the efflux rate of BC-NP in the 10–18 mesh soil-packed column rose from 4.24% to 29.17%, and the efflux rate of BC-NP increased from 1.49% to 14.19% when the background solution was 0.5 mM CaCl<sub>2</sub> (Table 1). These results are similar to the transport behavior of other nanoparticles (e.g., CeO<sub>2</sub> nanoparticles and silica nanoparticles) in saturated porous media (Li et al., 2017; Zhang et al., 2019). The difference was that in the presence of NaCl, the transportability of BC-NP increased with increasing HA concentration, but in the presence of CaCl<sub>2</sub>, the efflux rate of BC-NP was lower with 10 mg/L HA than that with 5 mg/L HA (Table 1).

Humic acid adsorbed on nanoparticles and the surface of collectors (soil particles) could cause an increase in the electrostatic repulsion among particles, affecting the stability of colloids and transport behavior of nanoparticles (Cao et al., 2022).

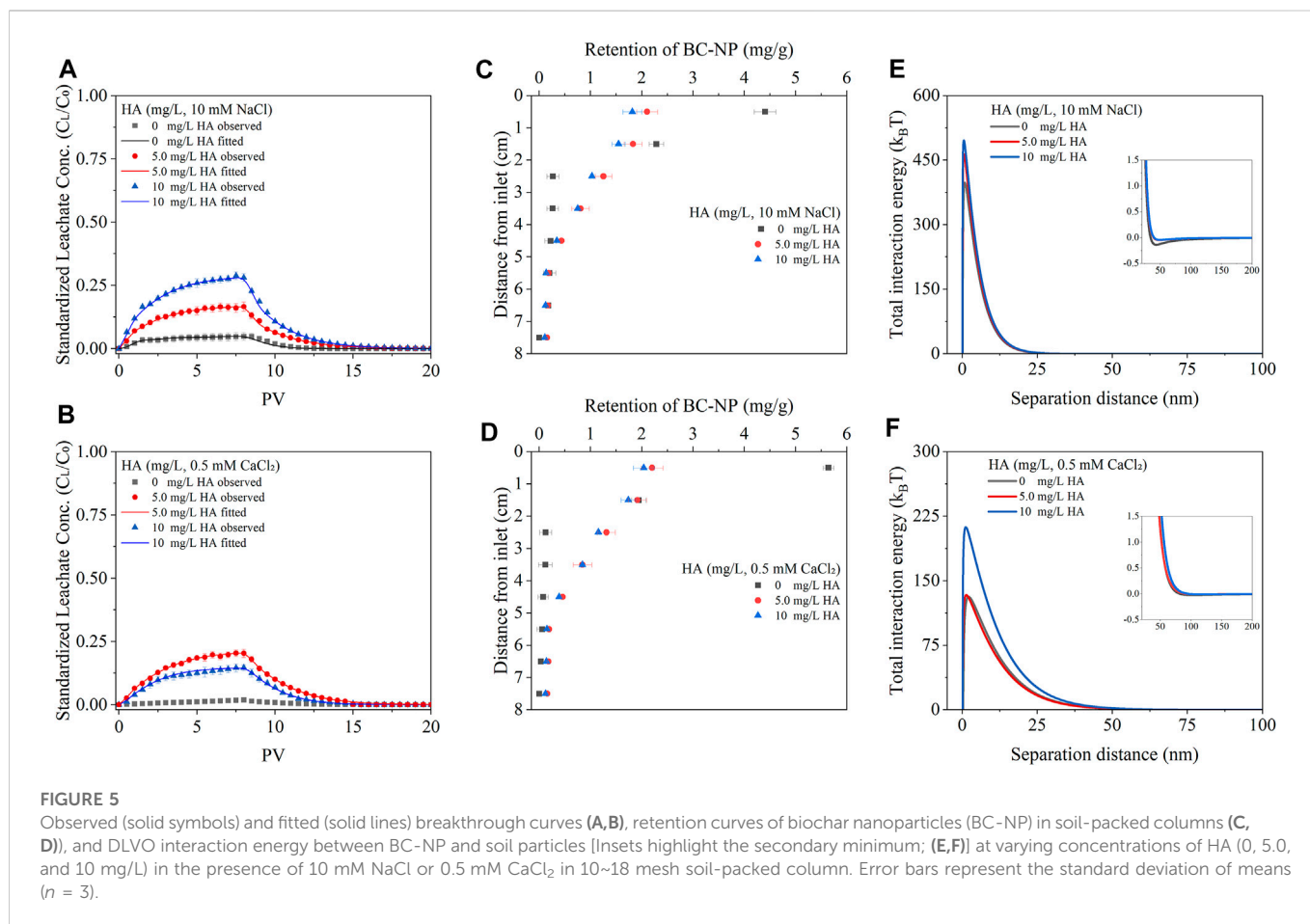


Previous reports suggested that HA could increase the absolute value of  $\zeta$ -potential of negatively charged colloids, which in turn could increase  $\Phi_{\max}$  between colloidal particles and porous media (Yang et al., 2017). In this study, the absolute  $\zeta$ -potential value of BC-NP and soil particles was higher in the presence of HA than in the absence of HA. For example, when HA concentration increased from 0 to 10 mg/L, the  $\zeta$ -potential of BC-NP in 10 mM NaCl solution decreased from -28.67 mV to -33.78 mV (Supplementary Table S5),  $\Phi_{\max}$  increased from 397.19 k<sub>B</sub>T to 495.84 k<sub>B</sub>T (Figure 5E and Supplementary Table S6). Soil particles also had a similar trend for  $\zeta$ -potential change (Supplementary Table S4). Thus, the increase in HA concentration enhanced the repulsion interaction energy between BC-NP and soil particles, creating unfavorable conditions for the solution chemistry-induced retention.

On the other hand, HA could considerably enhance the transportability of nanoparticles by masking porous media heterogeneity (e.g., positively charged iron and aluminum oxides sites in soil) or causing reversal of iron and aluminum oxides surface's charge from positive to negative (Ghosh et al., 2010). In this study, the difference between absolute  $\zeta$ -potential values of influx and efflux decreased gradually with increasing HA concentration. For example, when the background solution was 10 mM NaCl and 5 mg/L HA, the difference between the absolute  $\zeta$ -potential of the influx and the efflux was 8.13 mV. In contrast, when the concentration of HA increased to 10 mg/L, the value decreased to 6.79 mV (Supplementary Table S5). This showed

that charge competition and HA covered up the heterogeneity of soil particle surfaces and simultaneously affected the transportability of BC-NP in soil, suggesting that BC-NP with large absolute  $\zeta$ -potential value were adsorbed on positively charged clay minerals or metal oxides in the soil. In addition, during the transport of BC-NP, some HA molecules coated on BC-NP surface might be released and re-adsorbed on soil particles, further concealing the heterogeneity of soil surface charge (Chen et al., 2017). When HA was added to the background solution, heterogeneity of soil surface charge was partly masked, and the adsorption BC-NP on soil particles having increased negative charge was reduced. As a result, high transportability of BC-NP exhibited in the presence of HA.

When NaCl was used as the electrolyte, in the range of HA concentrations investigated here, the above effect was enhanced with increasing HA concentration. However, when a certain concentration of Ca<sup>2+</sup> and HA coexist, the bridging effect of Ca<sup>2+</sup> could promote the aggregation of nanoparticles, resulting in a decrease in the transportability of nanoparticles in porous media (Wang et al., 2015). For example, when the background solution was 0.5 mM CaCl<sub>2</sub> and 5 mg/L HA, the efflux rate of BC-NP was 20.78%, whereas the efflux rate of BC-NP was 14.19% when the background solution was 0.5 mM CaCl<sub>2</sub> and 10 mg/L HA (Table 1). This effect would depend on the increasing electrostatic repulsion caused by the presence of HA and the relative strength of the Ca<sup>2+</sup> bridging effect. In this study, the stability of BC-NP in suspension did not increase with HA



concentration, which also confirmed the above viewpoint (Figure 1D).

RC show a decreasing trend with soil depth, and the retention rate of BC-NP in the surface soil was the largest in the soil-packed columns with different HA concentrations (Figures 5C, D). Due to the size-exclusion effect, BC-NP with large grain sizes were more likely to remain in the soil than BC-NP with small grain sizes (Karaca et al., 2004; Wang et al., 2015). The hydrodynamic radius of BC-NP in the efflux was smaller than in the influx (Supplementary Table S5), which supported the above viewpoint. Furthermore, the  $\Phi_2$  min values increased notably with increasing HA concentration from 0 to 10 mg/L (Supplementary Table S6), indicating that secondary minimum retention was involved in the reduction of BC-NP retention with increasing HA concentration. The addition of HA also did not significantly change  $D_p/D_s$  and all of them were lower than 0.002 (Supplementary Table S4), indicating that straining had an insignificant effect on the retention of BC-NP in the presence of HA (Bradford et al., 2002; Fang et al., 2009).

Steric hindrance energy could also be an important factor affecting the transport of nanoparticles in porous media (Pelley and Tufenkji, 2008; Chen et al., 2012). However, predicting the thickness of HA coating on BC-NP and soil particles is difficult, hence the steric hindrance energy between BC-NP and soil particles was not considered in the DLVO interaction energy calculations. Previous studies suggested that the steric hindrance energy increased with increasing HA concentration, promoting the transport of nanoparticles in porous media (Chen et al., 2012). In this study,

HA affected the transport of BC-NP in soil by increasing electrical double layers repulsion, reducing the heterogeneity of soil surface charge, and possibly also through steric hindrance energy.

### 3.6 Transport modeling of BTC

The two-site kinetic retention model well described the BTC of BC-NP in this study (Figures 2, 5A, B), allowing to calculate and compare the model parameters [ $k_1$ ,  $k_{1d}$ ,  $k_{2str}$ ,  $S_{2max}$ , and Pearson's correlation coefficient ( $R^2$ )] among treatments and further discuss the BC-NP transport mechanisms.

For a given soil grain size,  $k_{1d}/k_1$  decreased gradually with the increase of cationic concentration and valence state in the background solution. For example, in the 10–18 mesh soil-packed column, when NaCl concentration increased from 1.0 mM to 50 mM, the  $k_{1d}/k_1$  value decreased from 0.688 to 0.668 (Table 2). Results showed that the electrostatic repulsions with increasing cationic concentration decreased based on the DLVO interaction energy calculations, resulting in a decreased reversible dissection at site 1 (e.g., negatively charged soil particles) (Chen et al., 2017). On the contrary,  $k_2$  and  $S_{2max}$  values increased with increasing cationic concentration, confirming that high cationic concentration could increase the retention rate of BC-NP in soil (Table 2). For a given cationic concentration and type, with decreasing soil grain size, the values of  $k_2$  and  $S_{2max}$  gradually increased, and retention of BC-NP in the soil also increased. This was due to the increase of specific surface

area and corresponding deposition location of the collector with decreasing collector (soil particles) size (Kasel et al., 2013; Sun et al., 2015).

When the background solution was 10 mM NaCl, the  $k_2$  and  $S_{2max}$  values decreased with the increase of HA concentration (Table 2). This was due to the fact that HA reduced the heterogeneity of soil surface charge (Ghosh et al., 2010) and increased the electrostatic repulsion between biochar nanoparticles and soil particles. Thus, as the HA concentration increased, the sites on the soil surface that were favorable for the deposition of BC-NP decreased. However, when the background solution was 0.5 mM  $CaCl_2$ , the  $k_2$  and  $S_{2max}$  values did not increase with an increase of HA concentration. For example, the  $k_2$  and  $S_{2max}$  values at 10 mg/L HA were 0.083 and 49.349, which were higher than 0.073 and 38.345 at 5 mg/L HA (Table 2). This may be due to the enhancement of  $Ca^{2+}$  bridging with the increase of HA

concentration (Wang et al., 2015), resulting in the inhibition of BC-NP transport and decreased  $k_2$  and  $S_{2max}$  values.

### 3.7 Implications for transport of BC-NP in soil matrix

It should be emphasized that the information obtained from the studies of BC-NP's transportability in model porous media (e.g., quartz sand) may amplify the transportability and risk of BC-NP in real soil matrix. For example, when 1.0 mM NaCl was used as the background solution,  $C_1/C_0$  (79.50%) of BC-NP transport through quartz sand (grain size, 425–600  $\mu m$ ) was much higher than that (38.20%) of BC-NP transport through soil (18–35 mesh, 425–880  $\mu m$ ) in the present study (Table 1). Compared with quartz sand, the larger

TABLE 2 Fitted parameters of the two-site kinetic retention model estimated for soil-packed columns at different experimental conditions.

Exp No. <sup>a</sup>	$k_1^b$	$k_{1d}^c$	$k_{1d}/k_1$	$k_2^d$	$S_{2max}^e$	$R^{2f}$
	( $min^{-1}$ )	( $min^{-1}$ )		( $min^{-1}$ )	(mg/g)	
1	0.753	0.518	0.688	0.060	10.395	.998
2	0.919	0.621	0.676	0.172	328.981	.967
3	0.472	0.315	0.668	0.196	344.346	.979
4	0.739	0.546	0.738	0.062	23.494	.983
5	— <sup>g</sup>	—	—	—	—	—
6	—	—	—	—	—	—
7	0.830	0.559	0.673	0.067	40.280	.986
8	—	—	—	—	—	—
9	—	—	—	—	—	—
10	0.837	0.585	0.699	0.070	56.651	.989
11	—	—	—	—	—	—
12	—	—	—	—	—	—
13	0.905	0.588	0.650	0.079	59.036	.991
14	—	—	—	—	—	—
15	—	—	—	—	—	—
16	0.852	0.540	0.634	0.084	64.358	.981
17	—	—	—	—	—	—
18	—	—	—	—	—	—
19	0.878	0.683	0.778	0.064	41.438	.996
20	1.006	0.807	0.803	0.059	33.647	.986
21	0.919	0.764	0.831	0.073	38.345	.991
22	0.869	0.685	0.789	0.083	49.349	.989

<sup>a</sup>The experimental numbers (Exp. No.) have the same condition as shown in Table 1.

<sup>b</sup>First-order attachment rate coefficient on the site 1.

<sup>c</sup>First-order detachment rate coefficient on the site 1.

<sup>d</sup>First-order attachment rate coefficient on the site 2.

<sup>e</sup>Maximum solid-phase concentration of BC-NP on the site 2.

<sup>f</sup>Pearson's correlation coefficient.

<sup>g</sup>Not determined.

surface area, heterogeneity of surface charge and surface roughness of paddy soil can explain the above phenomena. Researchers reported that the specific surface area of paddy soil was larger than that of clean quartz sand, providing more favorable retention sites for BC-NP (Chen et al., 2017). Furthermore, the positively charged metal oxides (iron and aluminum oxides) and the positively charged edges of clay minerals in the soil can hinder negatively charged BC-NP (Wang et al., 2014b). Additionally, soil particles with higher roughness can increase the favorable retention sites for BC-NP in both primary and secondary minimum (Shen et al., 2011; Chen et al., 2017).

In the present study, the efflux rate of BC-NP was 0.20%–67.17% (Table 1), indicating that some BC-NP would transport to the deeper soil (>8 cm) in the real soil matrix. However, compared with the uniformly filled soil in this study, the soil in the field has greater spatial heterogeneity. In general, open soil structures (e.g., cracks, fissures, worm trails, and other open features) (Jaisi and Elimelech, 2009) and soil organic matter (e.g., HA) (Chen et al., 2017), which can facilitate the transport of BC-NP, will decrease with an increase of soil profile depth. Therefore, we can speculate that the transportability of BC-NP in deep soil is lower than that in topsoil, and BC-NP may not always pose a risk in contaminating underlying groundwater aquifers. Moreover, BC-NP in real soil matrix may be more aggregated than the treated (stirred and sonicated) BC-NP used in this study, which would further enhance their retention in soils.

## 4 Conclusion

Through a large number of soil-packed column experiments, this study investigated the effects of ionic strength and soil grain size on the transport and retention of BC-NP in soil, which has great significance for the utilization of biochar in agricultural soil. Results showed that the transportability of BC-NP in columns with small soil grain size was lower than that in columns with large soil grain size, which could be attributed to mass transfer rate between BC-NP and soil particles and the straining effect. At low cation concentrations, the transportability of BC-NP in the soil was higher than at high cation concentrations. Due to a stronger charge neutralization ability than  $\text{Na}^+$ ,  $\text{Ca}^{2+}$  was more effective in inhibiting BC-NP transport than  $\text{Na}^+$ . Existence of natural organic compounds such as HA enhanced the transportability of BC-NP in the soil. Due to low electrical conductivity and high organic matter contents in most natural paddy soils, BC-NP may migrate over a long distance, adversely affecting soil nutrient availability and groundwater quality. In paddy soils that are rich in  $\text{Ca}^{2+}$  and lack organic matter, BC-NP can be retained in the soil profile, promoting carbon sequestration and nutrient conservation.

## References

- Adamczyk, Z., Siwek, B., Zembala, M., and Belouschek, P. (1994). Kinetics of localized adsorption of colloid particles. *Adv. Colloid Interface Sci.* 48, 151–280. doi:10.1016/0001-8686(94)80008-1
- Bradford, S. A., and Leij, F. J. (2018). Modeling the transport and retention of polydispersed colloidal suspensions in porous media. *Chem. Eng. Sci.* 192, 972–980. doi:10.1016/j.ces.2018.08.037
- Bradford, S. A., Simunek, J., Bettahar, M., Van Genuchten, M. T., and Yates, S. R. (2003). Modeling colloid attachment, straining, and exclusion in saturated porous media. *Environ. Sci. Technol.* 37, 2242–2250. doi:10.1021/es025899u

## Data availability statement

The original contributions presented in the study are included in the article/Supplementary Material, further inquiries can be directed to the corresponding authors.

## Author contributions

WZ and JM: conceptualization, methodology, software, writing—reviewing and editing. HW, BS, and BPS: writing—review and Editing. YH and YT: data curation, writing—original draft preparation. XZ and JG: visualization, investigation. WC: supervision, resources.

## Funding

This study was financially supported by the Science and Technology Plan Project of Shenyang, China (22-317-2-08; 2021-57), the earmarked fund for China Agriculture Research System (CARS01-51), the Innovative Talents Promotion Plan of Ministry of Science and Technology of the People's Republic of China (No. 2017RA2211).

## Conflict of interest

The authors declare that the research was conducted in the absence of any commercial or financial relationships that could be construed as a potential conflict of interest.

## Publisher's note

All claims expressed in this article are solely those of the authors and do not necessarily represent those of their affiliated organizations, or those of the publisher, the editors and the reviewers. Any product that may be evaluated in this article, or claim that may be made by its manufacturer, is not guaranteed or endorsed by the publisher.

## Supplementary material

The Supplementary Material for this article can be found online at: <https://www.frontiersin.org/articles/10.3389/fenvs.2022.1114940/full#supplementary-material>

- Bradford, S. A., Yates, S. R., Bettahar, M., and Simunek, J. (2002). Physical factors affecting the transport and fate of colloids in saturated porous media. *Water Resour. Res.* 38, 63-1–63-12. doi:10.1029/2002wr001340

- Braun, A., Klumpp, E., Azzam, R., and Neukum, C. (2015). Transport and deposition of stabilized engineered silver nanoparticles in water saturated loamy sand and silty loam. *Sci. Total Environ.* 535, 102–112. doi:10.1016/j.scitotenv.2014.12.023

- Cao, G., Qiao, J., Ai, J., Ning, S., Sun, H., Chen, M., et al. (2022). Systematic research on the transport of ball-milled biochar in saturated porous media: Effect of humic acid, ionic strength, and cation types. *Nanomaterials* 12, 988. doi:10.3390/nano12060988

- Chen, H., Gao, Y., Li, J., Fang, Z., Bolan, N., Bhatnagar, A., et al. (2022). Engineered biochar for environmental decontamination in aquatic and soil systems: A review. *Carbon Res.* 1, 4. doi:10.1007/s44246-022-00005-5
- Chen, L., Sabatini, D. A., and Kibbey, T. C. (2012). Transport and retention of fullerene (nC<sub>60</sub>) nanoparticles in unsaturated porous media: Effects of solution chemistry and solid phase coating. *J. Contam. Hydrol.* 138–139, 104–112. doi:10.1016/j.jconhyd.2012.06.009
- Chen, M., Wang, D., Yang, F., Xu, X., Xu, N., and Cao, X. (2017). Transport and retention of biochar nanoparticles in a paddy soil under environmentally-relevant solution chemistry conditions. *Environ. Pollut.* 230, 540–549. doi:10.1016/j.envpol.2017.06.101
- Chen, W., Meng, J., Han, X., Lan, Y., and Zhang, W. (2019). Past, present, and future of biochar. *Biochar* 1, 75–87. doi:10.1007/s42773-019-00008-3
- Faibish, R. S., Elimelech, M., and Cohen, Y. (1998). Effect of electrostatic double layer interactions on pfcine in cmiltration of colloidal suspensions: An experimental investigation. *J. Colloid Interface Sci.* 204, 77–86. doi:10.1006/jcis.1998.5563
- Fang, J., Shan, X., Wen, B., Lin, J., and Owens, G. (2009). Stability of titania nanoparticles in soil suspensions and transport in saturated homogeneous soil columns. *Environ. Pollut.* 157, 1101–1109. doi:10.1016/j.envpol.2008.11.006
- Feriancikova, L., and Xu, S. (2012). Deposition and remobilization of graphene oxide within saturated sand packs. *J. Hazard. Mat.* 235–236, 194–200. doi:10.1016/j.jhazmat.2012.07.041
- Ghosh, S., Mashayekhi, H., Bhowmik, P., and Xing, B. (2010). Colloidal stability of Al<sub>2</sub>O<sub>3</sub> nanoparticles as affected by coating of structurally different humic acids. *Langmuir* 26, 873–879. doi:10.1021/la902327q
- Gui, X., Song, B., Chen, M., Xu, X., Ren, Z., Li, X., et al. (2021). Soil colloids affect the aggregation and stability of biochar colloids. *Sci. Total Environ.* 771, 145414. doi:10.1016/j.scitotenv.2021.145414
- Ippolito, J. A., Cui, L. Q., Kammann, C., Wrage-Monnig, N., Estavillo, J. M., Fuertes-Mendizabal, T., et al. (2020). Feedstock choice, pyrolysis temperature and type influence biochar characteristics: A comprehensive meta-data analysis review. *Biochar* 2, 421–438. doi:10.1007/s42773-020-00067-x
- Jaisi, D. P., and Elimelech, M. (2009). Single-walled carbon nanotubes exhibit limited transport in soil columns. *Environ. Sci. Technol.* 43, 9161–9166. doi:10.1021/es1001927y
- Kamrani, S., Rezaei, M., Kord, M., and Baalousha, M. (2018). Transport and retention of carbon dots (CDs) in saturated and unsaturated porous media: Role of ionic strength, pH, and collector grain size. *Water Res.* 133, 338–347. doi:10.1016/j.watres.2017.08.045
- Karaca, S., Gurses, A., Ejder, M., and Acikyildiz, M. (2004). Kinetic modeling of liquid-phase adsorption of phosphate on dolomite. *J. Colloid Interface Sci.* 277, 257–263. doi:10.1016/j.jcis.2004.04.042
- Kasel, D., Bradford, S. A., Simunek, J., Heggen, M., Vereecken, H., and Klumpp, E. (2013). Transport and retention of multi-walled carbon nanotubes in saturated porous media: Effects of input concentration and grain size. *Water Res.* 47, 933–944. doi:10.1016/j.watres.2012.11.019
- Li, Z., Sahle-Demessie, E., Aly Hassan, A., Pressman, J. G., Sorial, G. A., and Han, C. (2017). Effects of source and seasonal variations of natural organic matters on the fate and transport of CeO<sub>2</sub> nanoparticles in the environment. *Sci. Total Environ.* 609, 1616–1626. doi:10.1016/j.scitotenv.2017.07.154
- Lian, F., Yu, W., Zhou, Q., Gu, S., Wang, Z., and Xing, B. (2020). Size matters: Nano-biochar triggers decomposition and transformation inhibition of antibiotic resistance genes in aqueous environments. *Environ. Sci. Technol.* 54, 8821–8829. doi:10.1021/acs.est.0c02227
- Liang, Y., Bradford, S. A., Simunek, J., Vereecken, H., and Klumpp, E. (2013). Sensitivity of the transport and retention of stabilized silver nanoparticles to physicochemical factors. *Water Res.* 47, 2572–2582. doi:10.1016/j.watres.2013.02.025
- Liang, Y., Luo, Y., Lu, Z., Klumpp, E., Shen, C., and Bradford, S. A. (2021). Evidence on enhanced transport and release of silver nanoparticles by colloids in soil due to modification of grain surface morphology and co-transport. *Environ. Pollut.* 276, 116661. doi:10.1016/j.envpol.2021.116661
- Liu, K., Ran, Q., Li, F., Shaheen, S. M., Wang, H., Rinklebe, J., et al. (2022). Carbon-based strategy enables sustainable remediation of paddy soils in harmony with carbon neutrality. *Carbon Res.* 1, 12. doi:10.1007/s44246-022-00012-6
- Liu, Y., Sun, H., Sun, J., Meng, X., Jiang, Y., and Wang, N. (2021). Transport of micro/nano biochar in quartz sand modified by three different clay minerals. *Environ. Pollut. Bioavailab.* 33, 113–121. doi:10.1080/26395940.2021.1932605
- Lozano, P., and Berge, N. D. (2012). Single-walled carbon nanotube behavior in representative mature leachate. *Waste Manage.* 32, 1699–1711. doi:10.1016/j.wasman.2012.03.019
- Mlih, R., Liang, Y., Zhang, M., Tombacz, E., Bol, R., and Klumpp, E. (2022). Transport and retention of poly (acrylic acid-co-maleic acid) coated magnetite nanoparticles in porous media: Effect of input concentration, ionic strength and grain size. *Nanomaterials* 12, 1536. doi:10.3390/nano12091536
- Morrisson, A. R., Park, J. S., and Sharp, B. L. (1990). Application of high-performance size-exclusion liquid chromatography to the study of copper speciation in waters extracted from sewage sludge treated soils. *Analyst* 115, 1429–1433. doi:10.1039/an9901501429
- Naghdi, M., Taheran, M., Pulicharla, R., Rouissi, T., Brar, S. K., Verma, M., et al. (2019). Pine-wood derived nanobiochar for removal of carbamazepine from aqueous media: Adsorption behavior and influential parameters. *Arab. J. Chem.* 12, 5292–5301. doi:10.1016/j.arabjc.2016.12.025
- Pelley, A. J., and Tufenkji, N. (2008). Effect of particle size and natural organic matter on the migration of nano- and microscale latex particles in saturated porous media. *J. Colloid Interface Sci.* 321, 74–83. doi:10.1016/j.jcis.2008.01.046
- Petosa, A. R., Jaisi, D. P., Quevedo, I. R., Elimelech, M., and Tufenkji, N. (2010). Aggregation and deposition of engineered nanomaterials in aquatic environments: Role of physicochemical interactions. *Environ. Sci. Technol.* 44, 6532–6549. doi:10.1021/es100598h
- Porubcan, A. A., and Xu, S. (2011). Colloid straining within saturated heterogeneous porous media. *Water Res.* 45, 1796–1806. doi:10.1016/j.watres.2010.11.037
- Ramanayaka, S., Vithanage, M., Alessi, D. S., Liu, W. J., Jayasundera, A. C. A., and Ok, Y. S. (2020). Nanobiochar: Production, properties, and multifunctional applications. *Environ. Sci. Nano* 7, 3279–3302. doi:10.1039/d0en00486c
- Shen, C., Li, B. G., Wang, C., Huang, Y., and Jin, Y. (2011). Surface roughness effect on deposition of nano- and micro-sized colloids in saturated columns at different solution ionic strengths. *Vadose Zone J.* 10, 1071–1081. doi:10.2136/vzj2011.0011
- Song, B., Chen, M., Zhao, L., Qiu, H., and Cao, X. (2019). Physicochemical property and colloidal stability of micron- and nano-particle biochar derived from a variety of feedstock sources. *Sci. Total Environ.* 661, 685–695. doi:10.1016/j.scitotenv.2019.01.193
- Sun, Y., Gao, B., Bradford, S. A., Wu, L., Chen, H., Shi, X., et al. (2015). Transport, retention, and size perturbation of graphene oxide in saturated porous media: Effects of input concentration and grain size. *Water Res.* 68, 24–33. doi:10.1016/j.watres.2014.09.025
- Swaren, L., Safari, S., Konhauser, K. O., and Alessi, D. S. (2022). Pyrolyzed biomass-derived nanoparticles: A review of surface chemistry, contaminant mobility, and future research avenues to fill the gaps. *Biochar* 4, 33. doi:10.1007/s42773-022-00152-3
- Tan, X. F., Liu, Y. G., Gu, Y. L., Xu, Y., Zeng, G. M., Hu, X. J., et al. (2016). Biochar-based nano-composites for the decontamination of wastewater: A review. *Bioresour. Technol.* 212, 318–333. doi:10.1016/j.biortech.2016.04.093
- Tian, Y., Gao, B., and Ziegler, K. J. (2011). High mobility of SDBS-dispersed single-walled carbon nanotubes in saturated and unsaturated porous media. *J. Hazard. Mat.* 186, 1766–1772. doi:10.1016/j.jhazmat.2010.12.072
- Torkzaban, S., Bradford, S. A., Van Genuchten, M. T., and Walker, S. L. (2008). Colloid transport in unsaturated porous media: The role of water content and ionic strength on particle straining. *J. Contam. Hydrol.* 96, 113–127. doi:10.1016/j.jconhyd.2007.10.006
- Wang, D., Ge, L., He, J., Zhang, W., Jaisi, D. P., and Zhou, D. (2014a). Hyperexponential and nonmonotonic retention of polyvinylpyrrolidone-coated silver nanoparticles in an Ultisol. *J. Contam. Hydrol.* 164, 35–48. doi:10.1016/j.jconhyd.2014.05.007
- Wang, D., Jaisi, D. P., Yan, J., Jin, Y., and Zhou, D. (2015). Transport and retention of polyvinylpyrrolidone-coated silver nanoparticles in natural soils. *Vadose Zone J.* 14, vzj2015.01.0007–13. doi:10.2136/vzj2015.01.0007
- Wang, D., Su, C., Zhang, W., Hao, X., Cang, L., Wang, Y., et al. (2014b). Laboratory assessment of the mobility of water-dispersed engineered nanoparticles in a red soil (Ultisol). *J. Hydrol.* 519, 1677–1687. doi:10.1016/j.jhydrol.2014.09.053
- Wang, D., Zhang, W., Hao, X., and Zhou, D. (2013). Transport of biochar particles in saturated granular media: Effects of pyrolysis temperature and particle size. *Environ. Sci. Technol.* 47, 821–828. doi:10.1021/es303794d
- Wang, P., Shi, Q., Liang, H., Steuerman, D. W., Stucky, G. D., and Keller, A. A. (2008). Enhanced environmental mobility of carbon nanotubes in the presence of humic acid and their removal from aqueous solution. *Small* 4, 2166–2170. doi:10.1002/sml.200800753
- Wang, Y., Wang, F., Xiang, L., Bian, Y., Wang, Z., Srivastava, P., et al. (2022). Attachment of positively and negatively charged submicron polystyrene plastics on nine typical soils. *J. Hazard. Mat.* 431, 128566. doi:10.1016/j.jhazmat.2022.128566
- Wang, Y., Zhang, W., Shang, J., Shen, C., and Joseph, S. D. (2019). Chemical aging changed aggregation kinetics and transport of biochar colloids. *Environ. Sci. Technol.* 53, 8136–8146. doi:10.1021/acs.est.9b00583
- Wu, P., Wang, Z., Bolan, N. S., Wang, H., Wang, Y., and Chen, W. (2021). Visualizing the development trend and research frontiers of biochar in 2020: A scientometric perspective. *Biochar* 3, 419–436. doi:10.1007/s42773-021-00120-3
- Wu, S., Cai, X., Liao, Z., He, W., Shen, J., Yuan, Y., et al. (2022). Redox properties of nano-sized biochar derived from wheat straw biochar. *RSC Adv.* 12, 11039–11046. doi:10.1039/d2ra01211a
- Wu, X., Lyu, X., Li, Z., Gao, B., Zeng, X., Wu, J., et al. (2020). Transport of polystyrene nanoplastics in natural soils: Effect of soil properties, ionic strength and cation type. *Sci. Total Environ.* 707, 136065. doi:10.1016/j.scitotenv.2019.136065
- Xin, J., Tang, F., Zheng, X., Shao, H., and Kolditz, O. (2016). Transport and retention of xanthan gum-stabilized microscale zero-valent iron particles in saturated porous media. *Water Res.* 88, 199–206. doi:10.1016/j.watres.2015.10.005

- Xin, X., Judy, J. D., Zhao, F., Goodrich, S. L., Sumerlin, B. S., Stoffella, P. J., et al. (2021). Transport and retention of polymeric and other engineered nanoparticles in porous media. *NanoImpact* 24, 100361. doi:10.1016/j.impact.2021.100361
- Xu, F., Wei, C., Zeng, Q., Li, X., Alvarez, P. J. J., Li, Q., et al. (2017). Aggregation behavior of dissolved barbon: Implications for vass flux and fquatic systems. *Environ. Sci. Technol.* 51, 13723–13732. doi:10.1021/acs.est.7b04232
- Yang, W., Shang, J., Sharma, P., Li, B., Liu, K., and Flury, M. (2019). Colloidal stability and aggregation kinetics of biochar colloids: Effects of pyrolysis temperature, cation type, and humic acid concentrations. *Sci. Total Environ.* 658, 1306–1315. doi:10.1016/j.scitotenv.2018.12.269
- Yang, W., Wang, Y., Shang, J., Liu, K., Sharma, P., Liu, J., et al. (2017). Antagonistic effect of humic acid and naphthalene on biochar colloid transport in saturated porous media. *Chemosphere* 189, 556–564. doi:10.1016/j.chemosphere.2017.09.060
- Yao, K., Habibian, M. T., and O'melia, C. R. (2002). Water and waste water filtration. Concepts and applications. *Environ. Sci. Technol.* 5, 1105–1112. doi:10.1021/es60058a005
- Zhang, M., Li, D., Ye, Z., Wang, S., Xu, N., Wang, F., et al. (2019). Effect of humic acid on the sedimentation and transport of nanoparticles silica in water-saturated porous media. *J. Soils Sediments* 20, 911–920. doi:10.1007/s11368-019-02444-x
- Zhang, Q., Wu, X., Lyu, X., Gao, B., Wu, J., and Sun, Y. (2022a). Effects of anionic hydrocarbon surfactant on the transport of perfluorooctanoic acid (PFOA) in natural soils. *Environ. Sci. Pollut. Res.* 29, 24672–24681. doi:10.1007/s11356-021-17680-3
- Zhang, X., Wells, M., Niazi, N.K., Bolan, N., Shaheen, S., Hou, D., et al. (2022b). Nanobiochar-rhizosphere interactions: Implications for the remediation of heavy-metal contaminated soils. *Environ. Pollut.* 299, 118810. doi:10.1016/j.envpol.2022.118810